symmetry

MDPI

Article

Estimation of Natural Radionuclides' Concentration of the Plutonic Rocks in the Sakarya Zone, Turkey Using Multivariate Statistical Methods

Fusun Yalcin [1], Nurdane Ilbeyli [2,*], Mehmet Demirbilek [3], Mustafa Gurhan Yalcin [2], Alper Gunes [2], Abdullah Kaygusuz [4] and Suleyman Fatih Ozmen [5]

1 Department of Mathematics, Akdeniz University, 07058 Antalya, Turkey; fusunyalcin@akdeniz.edu.tr
2 Department of Geological Engineering, Akdeniz University, 07058 Antalya, Turkey; gurhanyalcin@akdeniz.edu.tr (M.G.Y.); alpergunes@akdeniz.edu.tr (A.G)
3 Department of Geological Engineering, Dumlupinar University, 43100 Kutahya, Turkey; mehmet.demirbilek@dpu.edu.tr
4 Department of Geological Engineering, Gumushane University, 29100 Gumushane, Turkey; akaygusuz@gumushane.edu.tr
5 Department of Physics, Akdeniz University, 07058 Antalya, Turkey; fatihozmen@akdeniz.edu.tr
* Correspondence: ilbeyli@akdeniz.edu.tr; Tel.: +90-2423106376; Fax: +90-2423106306

Received: 3 May 2020; Accepted: 19 June 2020; Published: 23 June 2020

check for updates

Abstract: The study aimed to determine the natural radioactivity levels of ^{226}Ra, ^{232}Th, and ^{40}K by the Gamma-Ray spectrometry method, and radiological hazard parameters of the plutonic rocks in the Western and Central Sakarya Zone and to analyze the data using multivariate statistical methods. The average radiological values of samples were determined as ^{40}K (1295.3 Bq kg^{-1}) > ^{232}Th (132.1 Bq kg^{-1}) > ^{226}Ra (119.7 Bq kg^{-1}). According to the skewness values of the distributions of the examined radionuclides, ^{226}Ra (2.1) and ^{232}Th (0.7) seemed to be positively right-skewed while ^{40}K (−0.2) had a negatively right-skewed histogram. On the other hand, the following kurtosis values were calculated for the distributions: ^{226}Ra (5.8 > 3), ^{232}Th (−0.7), and ^{40}K (−0.8). Kolmogorov–Smirnov and Shapiro–Wilk tests were applied to the data to test their normality. Therefore, Spearman's correlation coefficient method was performed. The radionuclides of ^{226}Ra and ^{232}Th were found to have a positive correlation with radiological hazard parameters of the samples. 2 (two)-related factors identified, and the cumulative value was calculated to be 98.7% on the basis of the Scree Plot. According to the hierarchical cluster analysis, the samples that are grouped with those from Camlik region are prominent. The average radioactivity values of Camlik, Sogukpinar, Karacabey, and Sogut (except for ^{232}Th) regions were detected to be higher than the world averages while the value of ^{40}K was also found to be higher than the average values of various countries in the world.

Keywords: radioactivity; radiological hazard parameters; multivariate statistics; data analysis; plutonic rocks

MSC: 62H10; 62H86; 62H25; 62H30

1. Introduction

"Natural radioactivity" is observed all around the world, particularly in the geological environment consisting of rocks, soils, plants, fluids, and gas as well as the artificial environment consisting of man-made structures [1–9]. People living in environments containing natural radioactivity are exposed to different doses of radiation. People living in the natural environment receive 82% of their average annual dose (2.4 µSv) from natural radiation sources. Therefore, natural radiation sources are important for the health of people [9]. It is also important to learn the decay rates of radionuclides regarding these sources. Radioactive equilibrium is the state in which each radionuclide has the same decay. Understanding the decay chain equilibrium helps estimate the amount of radiation to be emitted in the decay of radionuclide. There are detailed studies on radioactive equilibrium, which is one of the important issues, in the literature [10]. The amount of radium (^{226}Ra), thorium (^{232}Th), and potassium (^{40}K) contents of the materials are measured to define natural radiation rates and to calculate radiological hazard indices. Radium (^{226}Ra), thorium (^{232}Th), and potassium (^{40}K) isotopes can be observed in various levels in plutonic rocks. Plutonic rocks and soils are among rocks with terrestrial and cosmic radiation, with high levels of natural radioactivity. Therefore, exposure to gamma rays may pose health risks for people [11–13]. These rocks that we contact in various ways are very crucial in terms of the health of living things.

Many locations in Turkey and around the world have been studied in terms of granitic rocks [14–38]. In the literature, there are studies on the plutonic rocks in the Northwestern and Western Anatolia (Ilica, Cataldag, Uludag, Eybek, Kozak, Evciler, Orhaneli, Kapidag, Camlik, Topuk, Tepeldag, Gurgenyayla, Egrigoz), which were partially covered by the study area [18,24]. However, no detailed and comprehensive study has been found in the literature on the specified locations in the Sakarya Zone, which is the study area, except for the Camlik region. The findings of the former studies increased the importance of the unstudied regions where the plutonic rocks spread. Therefore, the use of these rocks and the presence of habitats and residential areas in the study area increase the significance of this study.

In this context, the study aimed to measure the radioactivity levels of the plutonic rocks widely observed in the Sakarya Zone to determine the radiation hazard indices, and to interpret all the data obtained by using multivariate statistical analysis. Besides, interpretations were made by comparing the obtained data and the radiogenic levels exposed to living things in the regions with the values of different areas.

2. Materials and Methods

2.1. Description of the Study Area

The study area is located in the Sakarya Zone on which there are a few large and small settlements. The settlements in the study area have different names; therefore, the rock samples taken from different regions were given codes according to their locations. For example, a sample from Ericek was given the code of "ER" and recorded as "Sample No: ER"; similarly, other samples from Karacabey, Camlik, Sogut, Kapanca, and Sogukpinar were given the codes of "KR", "E", "F", "ST", "KP", and "SR", respectively. The villages where the rock samples were taken, and their vicinity are shown on the site location map (Figure 1).

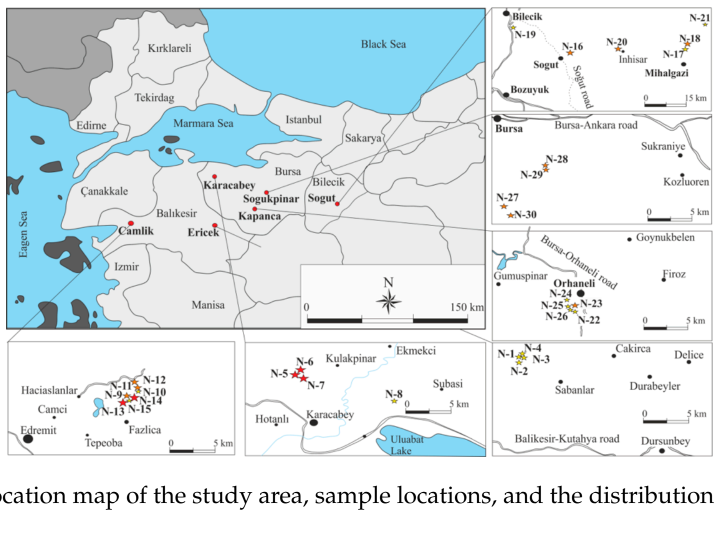

Figure 1. Site location map of the study area, sample locations, and the distribution of ^{40}K samples.

The region extending from the Biga Peninsula to the Eastern Pontides is called the Sakarya Zone, which is characterized by sedimentary and igneous rocks subjected to intense deformation and metamorphism in different facies [39]. There are igneous rocks of various ages and origins in the Sakarya Zone

2.2. Sampling and Preparation

A total of 30 rock samples were collected from the plutonic rocks in the study area and several locations where the regional rocks dominated. An area of approximately 100 m^2 was marked at each sampling location. After removing impurities, such as stones, pebbles, and roots, 50–100 g of rock samples were taken in each corner and center of the marked area to a depth of about 50 cm. Four different samples representing the study area were taken for each sample. The sub-samples obtained were mixed and put in packages of 400–500 g. The samples were packed in polyethylene bags, systematically labeled, and the coordinates of the sample locations were recorded using Global Positioning System (GPS). The samples were homogenized using an agate mortar at the sample preparation laboratory of the Department of Geological Engineering at Akdeniz University (Turkey) and kept under normal conditions in the laboratory environment for a month to achieve secular equilibrium.

All samples were kept tightly closed with gas-tight parafilm and stored for about 30 days to form a radioactive equilibrium between ^{226}Ra and ^{222}Rn and stabilize the Compton region (7 × 3.9 days) [40].

2.3. Radioactivity Measurements Using High-Purity Germanium (HPGe) Detector and Dose Calculations

The gamma spectroscopic measurements of the plutonic rock samples were performed with AMETEK-ORTEC brand, GEM40P4 model, High Purity Germanium (HPGe) detector and Maestro32 software at the Department of Physics at Akdeniz University (Turkey). The relative efficiency of the HPGe detector was 40%. The full width half maximum (FWHM) values at 122 keV (^{57}Co) and at 1332 keV (^{60}Co) were 768 eV and 1.85 keV, respectively. The energy and efficiency calibration of the HPGe gamma spectrometer were made using the mixed source (International Atomic Energy Agency, (IAEA) 1364-43-2) of the same geometry with sample energies ranging from 47 to 1836 keV. IAEA RGU-1, RGTh-1, and RGK-1 standards were used for the quality controls and activity calculations (Table 1). Detailed information about the measurement system is provided by [40,41].

Table 1. Summary of the analysis of standard materials.

Standard	Reference Value (Bq kg^{-1})	Measured Value (Bq kg^{-1})
RGU-1	4940 ± 30	4964 ± 72
RGTh-1	3250 ± 90	3276 ± 64
RGK-1	14000 ± 400	14240 ± 546

All samples were counted for 50,000 s. Background intensities were also obtained under the same conditions before and after the measurements of the samples. In the gamma spectra of the samples, the activity concentrations of ^{226}Ra were determined by using 352 (^{214}Pb) and 609 keV (^{214}Bi), while the activity concentrations of ^{232}Th were determined by using 911 (^{228}Ac) and 583 keV (^{208}Tl) energy peaks, which were released from product radionuclides in the ^{238}U and ^{232}Th disintegration series. ^{40}K activity concentrations were determined by using the 1461 keV energy peak. Radionuclide activity concentrations were calculated using Equation (1):

$$A = \frac{N/t}{\varepsilon \times I_{\gamma} \times m}, \quad (1)$$

where A stands for the activity of the radionuclide in Bq kg^{-1}, N stands for the total net count in the energy of interest as counting time in seconds, ε stands for the efficiency of the HPGe detector in the gamma energy of interest, I_γ stands for the abundance of the gamma ray, and m stands for the sample mass [40,41].

2.4. Radiation Hazards Parameters

Firstly, the samples of the radioactivity levels of the naturally occurring radionuclide materials (NORMs) collected from the study area were measured. Then, internationally adopted radiological health parameters were calculated using all of the data obtained by the gamma-ray spectrometry method (Table 2). Finally, multivariate statistical analyses were performed on all data obtained and the results were interpreted by comparing them with world averages.

Table 2. Radiological parameters.

S/N	Radiological Parameters	Units	Used Formula	References
1	Absorbed dose rate (D)	nGy hr^{-1}	D_R = (0.462 A_U + 0.604A_{Th} + 0.0417 A_K) ≤ 80	[14,36]
2	Radium equivalent (Ra_{eq})	Bq kg^{-1}	Ra_{eq} = (Au + 1.43 A_{Th} + 0.077 A_K) ≤ 370	[14,36]
3	Alfa index (Iα)	µRh r^{-1}	Iα = A_U/200 ≤ 1	[42]
4	Gamma index (Iγ)	-	Iγr = A_U/300 + A_{Th}/200 + A_K/3000 ≤ 1	[43]
5	External hazard index (H_{ex})	-	H_{ex} = A_U/370 + A_{Th}/259 + A_K/4810 ≤ 1	[44]
6	Internal hazard index (H_{in})	-	H_{in} = AU/185 + A_{Th}/259 + A_K/4810 ≤ 1	[42]
7	Annual effective dose equivalent ($AEDE_{indoor}$)	µSv yr^{-1}	$AEDE_{(indoor)}$ = D_R × 8766 h × 0.7 Sv/Gy × 0.8 × 10^{-3} ≤ 0.48	[14,36,42]
8	Annual effective dose equivalent ($AEDE_{outdoor}$)	µSv yr^{-1}	$AEDE_{(outdoor)}$= D_R × 8766 *h* × 0.7 *Sv/Gy* × 0.2 × 10^{-3} ≤ 0.48	[14,36]
9	Annual gonadal dose equivalent (AGDE)	µSv yr^{-1}	AGDE= 3.09 A_U × 4.18 A_{Th} × 0.314 A_K ≤ 300	[36,45]
10	Excess lifetime cancer risk ($ELCR_{outdoor}$)	µSv yr^{-1}	$ELCR_{(outdoor)}$ = $AEDE_{outdoor}$ × DL × RF ≤ 0.29	[35,46,47]
11	Activity utilization index (AUI)	-	AUI = A_U/50 f_U + A_{Th}/50 f_{Th} + A_K/500 f_K ≤ 2	[48]

Where A_U, A_{Th}, and A_K are the activity concentrations of ^{238}U, ^{232}Th, and ^{40}K in (Bq kg^{-1}) present in tar sand soil, respectively. f_U (0.462), f_{Th} (0.604), and f_K (0.0417) are the fractional contributions to the total dose rate due to γ-radiation from the actual radionuclide of ^{238}U, ^{232}Th, and ^{40}K, respectively. DL and RF is duration of life (70 years) and risk factor (Sv^{-1}), fatal cancer risk per Sievert. For stochastic effects, ICRP 60 uses values of 0.05 for the public.

The following radiological health parameters were applied to radioactivity levels: Absorbed dose rate (D), radium equivalent activity (Ra_{eq}), alfa index (Iα), gamma index (Iγ), external hazard index (H_{ex}), internal hazard index (H_{in}), annual effective dose equivalent ($AEDE_{indoor}$), annual effective dose equivalent ($AEDE_{outdoor}$), annual gonadal dose equivalent (AGDE), excess lifetime cancer risk ($ELCR_{outdoor}$), and activity utilization index (AUI).

2.5. Statistical Analysis

Multivariate statistical studies on the interpretation of radioactivity data and radiological parameters are quite important [49–51]. In this regard, multivariate statistical analyses are useful, and these tools are required to explain the data. In this study, multivariate statistical analyses, such as correlation analysis, factor analysis, cluster analysis, and regression analysis, were performed to interpret the data using the SPSS 23 software package.

2.6. Comparison with Other Countries

This finding of this study were compared with those of similar studies conducted in different parts of the world, and the differences between them were revealed.

3. Findings

3.1. Activity Concentration and Radiological Characterization

Table 3 gives the radiological health parameters calculated for the study area.

Table 3. Radiological parameters of the plutonic and metamorphic rock samples of the western and central Sakarya zone.

Locations	Number	Longitude	Latitude	Rock Types	^{226}Ra (Bq kg^{-1})	±	^{232}Th (Bq kg^{-1})	±	^{40}K (Bq kg^{-1})	±	D nGy hr^{-1}	Ra_{eq} Bq kg^{-1}	Iα μRhr $^{-1}$	Iγ	H_{ex}	H_{in}	$AEDE_{indoor}$ μSv yr^{-1}	$AEDE_{outdoor}$ μSv yr^{-1}	AGDE μSv yr^{-1}	ELCR μSv yr^{-1}	AUI
	N1-ER-2	28.432043098	39.676005958	Metagranite	12.11	0.81	9.33	0.73	39.26	2.03	12.87	28.47	0.06	0.10	0.08	0.11	63.16	15.79	88.74	55.26	0.23
Ericek	N2-ER-3	28.431755220	39.676180693	Chlorite schist	16.41	0.99	44.39	3.74	18.75	0.90	35.17	81.33	0.08	0.28	0.22	0.26	172.66	43.17	242.13	151.08	0.69
	N3-ER-4	28.431715042	39.675928916	Metagranite	9.84	0.70	0.00	0.00	99.35	3.80	8.69	17.49	0.05	0.07	0.05	0.07	42.65	10.66	61.59	37.32	0.10
	N4-ER-5	28.431291691	39.675753940	Metagranite	118.36	8.86	0.00	0.00	45.94	1.76	56.60	121.90	0.59	0.41	0.33	0.65	277.84	69.46	380.16	243.11	1.10
	N5-KR-1	28.324269802	40.273353542	Metagranite	39.18	3.32	66.84	3.15	1982.63	111.78	141.15	287.42	0.20	1.13	0.78	0.88	692.88	173.22	1022.99	606.27	1.33
Karacabey	N6-KR-3	28.327619381	40.278639427	Musqovite schist	141.97	8.83	126.70	6.96	2300.20	122.99	238.04	500.27	0.71	1.87	1.35	1.73	1168.51	292.13	1690.57	1022.45	3.03
	N7-KR-4	28.334002977	40.271881386	Metagranite	140.29	12.19	203.21	12.24	2026.38	78.34	272.05	586.91	0.70	2.16	1.59	1.96	1335.50	333.88	1919.20	1168.56	3.92
	N8-KR-7	28.467674661	40.252524554	Granite	133.31	10.46	147.12	11.33	1110.49	46.14	196.76	429.20	0.67	1.55	1.16	1.52	965.87	241.47	1375.58	845.13	3.10
	N9-F-29	27.147836611	39.654970995	Granite	337.78	24.65	366.98	18.60	2164.45	95.02	467.97	1029.23	1.69	3.68	2.78	3.69	2297.25	574.31	3257.37	2010.09	7.73
	N10-F-31	27.160345614	39.660657918	Dike	152.58	7.67	263.77	20.58	1160.89	57.31	278.22	619.17	0.76	2.21	1.67	2.08	1365.77	341.44	1938.57	1195.05	4.69
	N11-F-34	27.160405794	39.666523519	Granite	314.22	14.91	386.84	27.14	2158.89	88.00	468.85	1033.64	1.57	3.70	2.79	3.64	2301.56	575.39	3265.84	2013.86	7.76
Camlik	N12-F-35A	27.157165668	39.677241137	Granite	353.71	23.43	381.28	25.06	2323.22	89.28	490.59	1077.83	1.77	3.86	2.91	3.87	2408.26	602.07	3416.20	2107.23	8.07
	N13-E-3	27.141680038	39.648329069	Aplite	425.80	29.54	351.98	31.85	3569.09	162.79	558.15	1203.96	2.13	4.37	3.25	4.40	2739.93	684.98	3907.71	2397.44	8.48
	N14-E-14	27.153147118	39.652747590	Pegmatite	752.30	50.70	367.90	17.46	2921.97	130.26	691.62	1503.39	3.76	5.32	4.06	6.09	3395.14	848.79	4779.93	2970.75	11.64
	N15-E-18	27.148632065	39.650834260	Granite	295.53	15.30	285.12	18.10	1689.39	85.85	379.20	833.34	1.48	2.97	2.25	3.05	1861.46	465.36	2635.47	1628.78	6.32
	N16-ST-1	30.221631828	40.034862141	Metagranite	151.35	11.15	113.01	9.74	1924.67	110.23	218.44	461.15	0.76	1.71	1.25	1.65	1072.30	268.07	1544.37	938.26	2.92
	N17-ST-52	30.583316796	40.069253317	Granite	50.41	2.55	82.25	5.65	1694.93	81.92	143.65	298.54	0.25	1.14	0.81	0.94	705.17	176.29	1031.79	617.02	1.60
Sogut	N18-ST-59	30.588577067	40.081668280	Pegmatite	83.98	4.33	99.68	5.22	2221.42	88.19	191.64	397.57	0.42	1.52	1.07	1.30	940.74	235.19	1373.68	823.15	2.17
	N19-ST-80	30.011660747	40.093298000	Metagranite	50.75	3.98	79.35	6.75	1569.46	78.43	136.82	285.07	0.25	1.09	0.77	0.91	671.66	167.91	981.33	587.70	1.56
	N20-ST-87	30.383392504	40.042351196	Metagranite	140.83	12.93	117.24	8.57	1975.17	91.55	218.24	460.57	0.70	1.71	1.24	1.62	1071.34	267.84	1545.44	937.43	2.88
	N21-ST-89	30.728501362	40.137206230	Diorite	4.36	0.23	7.11	0.40	568.24	22.08	30.00	58.28	0.02	0.24	0.16	0.17	147.28	36.82	221.60	128.87	0.17
	N22-KP-1	28.972752904	39.888305934	Metagranite	9.70	0.48	30.97	2.15	623.95	29.57	49.21	102.03	0.05	0.40	0.28	0.30	241.55	60.39	355.34	211.35	0.52
	N23-KP-2	28.970348655	39.890517980	Pegmatite	60.63	5.08	195.26	10.36	2582.37	147.27	253.63	538.69	0.30	2.04	1.45	1.62	1245.07	311.27	1814.39	1089.43	3.13
Kapanca	N24-KP-8	28.965301549	39.895612630	Granite	21.78	1.29	14.93	0.71	545.25	31.45	41.82	85.12	0.11	0.33	0.23	0.29	205.28	51.32	300.92	179.62	0.43
	N25-KP-11	28.969088271	39.889386245	Granite	41.52	2.67	41.22	2.53	10.47	0.47	44.52	101.27	0.21	0.35	0.27	0.39	218.53	54.63	303.89	191.21	0.88
	N26-KP-12	28.967971372	39.891225020	Granite	40.11	2.70	50.67	4.52	343.10	13.97	63.44	138.98	0.20	0.50	0.38	0.48	311.42	77.86	443.45	272.49	1.01
	N27-SR-5	29.109736537	40.073022948	Metagranite	106.13	9.41	153.35	8.01	2099.64	105.49	229.21	487.10	0.53	1.82	1.32	1.60	1125.20	281.30	1628.25	984.55	3.01
Sogukpinar	N28-SR-11	29.153432195	40.122621203	Metagranite	209.55	17.49	215.89	10.78	2061.64	77.85	313.18	677.02	1.05	2.47	1.83	2.39	1537.39	384.35	2197.29	1345.22	4.72
	N29-SR-12	29.153432195	40.122621203	Metagranite	119.06	7.29	136.83	9.29	2134.53	85.91	226.66	479.09	0.60	1.79	1.29	1.62	1112.67	278.17	1610.09	973.58	2.93
	N30-SR-18	29.118678516	40.064157408	Granite	122.31	8.34	104.17	6.33	2012.03	102.53	203.33	426.20	0.61	1.60	1.15	1.48	998.14	249.53	1445.16	873.37	2.56

The recommended average value of the gamma radiation absorbed dose rate (D) ranges between 10 and 200 nGy hr^{-1}, and the population-weighted gamma radiation absorbed dose rate is 59 nGy hr^{-1} [14]. D values of the samples were observed to range between 8.7 and 691.6 nGy hr^{-1} and the mean value was found to be 222 nGy hr^{-1}. The maximum and average absorbed dose rates due to gamma radiation in the air 1 m above the ground level exceeded world limit values. Moreover, these values are well above the limit value that should be taken into account in the settlements.

The limit value for radium equivalent activity (Ra_{eq}) ranges between 370 and 740 Bg kg^{-1} [14]. Ra_{eq} values, which were calculated to identify the homogeneous distributions of radionuclides, were observed between 17.5 and 1503.4 Bg kg^{-1} with an average value of 478.3 Bg kg^{-1}. The maximum and average values were observed to exceed world limits.

The recommended limit value for the alpha index ($I\alpha$) is $I\alpha < 1$ μRh r^{-1} [14]. $I\alpha$ values were calculated to be between 0.02 and 3.8 μRh r^{-1} with an average value of 0.7 μRh r^{-1}. The maximum value exceeded the recommended limit values. According to the average values, no problems were observed in terms of radon inhalation; however, there seemed a problem according to the maximum value.

While the recommended upper limit for gamma index ($I\gamma$) is $I\gamma < 1$ μRh r^{-1}, the exemption criterion of gamma dosage is $I\gamma < 0.3$ μRh r^{-1} [14]. In this study, $I\gamma$ values were observed to range between 0.07 and 5.3 μRh r^{-1} with an average of 1.8 μRh r^{-1}. The maximum $I\gamma$ value exceeded the recommended upper limit. The samples with a maximum value exceeding $I\gamma < 0.3$ μRh r^{-1} are not suitable to be used as a building material. The radiological effect must be at least ($I\gamma < 0.5$) to be tolerated.

The external hazard index (H_{ex}) was calculated together with the internal hazard index (H_{in}) to evaluate the effects of the radioactivity of the surface materials on health. The recommended limit value for the external hazard index (H_{ex}) is ($H_{ex} < 1$). In the study, Hex values were observed to be between 0.05 and 4.1 with an average of 1.3. The maximum and average values were found to exceed the limit values.

The recommended limit value for the internal alpha radiation (H_{in}) is $H_{in} < 1$ [14]. In the study, H_{in} values were found to range between 0.07 and 6.1, with an average of 1.7. All values were observed to exceed the limit value. According to these figures, health problems stemming from the inhalation of radon and radon products can be seen. The radiological hazard indices of the samples should be below the limit values ($H_{ex} < 1$ and $H_{in} < 1$) to assume their radiological effects are not significant.

The recommended world average for the annual effective dose equivalent (AEDE) is AEDE < 70 μSv yr^{-1} [14]. The minimum, maximum, and mean values of $AEDE_{indoor}$ and $AEDE_{outdoor}$ were calculated to be 42.7–3395.1 μSv yr^{-1}, 1089.7 μSv yr^{-1} (mean) and 10.7–848.8 μSv yr^{-1}, and 272.4 μSv yr^{-1} (mean), respectively. The samples were observed to have high $AEDE_{indoor}$ values. The maximum and mean values were found to exceed limit values. The regions seem to have a health problem of inhalation of radon and its products.

The recommended limit for the annual gonadal dose equivalent (AGDE) is AGDE < 300 μSv yr^{-1} [14]. An active cell's direct exposure to radiation may damage the reproductive organs, active bone marrow, and bone surface cells; it may even lead to cell mutation or death [14,52,53]. In this study, the AGDE values ranged between 61.6 and 4779.9 μSv yr^{-1}, and the average AGDE was observed to be 1559.3 μSv yr^{-1}. The maximum and average AGDE values were found to exceed the limit values. These findings are significant since the radiation taken by the reproductive organs (gonads) of the population exceeds the recommended annual dose equivalent.

The recommended limit value for the excess lifetime cancer risk ($ELCR_{outdoor}$) is $ELCR_{outdoor} < 2.9 \times 10^{-4}$ μSv yr^{-1} [14]. The $ELCR_{outdoor}$ values were found to range between 37.3 and 2970.8 (μSv yr^{-1}) with an average of 953.5. μSv yr^{-1}. All values were observed to be well above the limit value. According to these results, the lifetime cancer risk of the people who live in these regions with anomalies for up to 70 years due to land use is quite high. Therefore, the contact of people living in these regions with these plutonic rocks in their living areas should be reduced.

If the recommended limit value for the activity utilization index (AUI) is AUI ≤ 1, the dose that the individual receives corresponds to 0.3 μSv yr^{-1}. On the other hand, if the limit value is AUI ≤ 3, the dose that the individual receives corresponds to 1 μSv yr^{-1} [14]. In this study, the AUI values were observed to range between 0.1 and 11.6 μSv yr^{-1} with an average of 3.3 μSv yr^{-1}. Since the maximum and average values exceeded the limit value (AUI ≤ 3), the regions were found to have excess amounts of external gamma radiation (1 μSv yr^{-1}) due to the surface materials.

The regions in the study area from where the samples with the maximum and average values exceeding the international limit values were taken may pose significant radiological risks to the people living there.

3.2. Multivariate Statistical Analysis and Data Mining

3.2.1. Descriptive Statistics

Descriptive statistical analyses were applied to radiological indices calculated by the radiological analyses and the data obtained from them (Table 4). The mean values of the radionuclides obtained by radiological analyses were ordered as follows: ^{40}K (1532.6 Bq kg^{-1}) > ^{226}Ra (148.5 Bq kg^{-1}) > ^{232}Th (148.1 Bq kg^{-1}). It is noteworthy that the values of ^{226}Ra and ^{32}Th are close to each other, and they show a similar concentration. This indicates that these radionuclides showed similar behavior and that they are not affected by the metamorphism of the rocks. The samples were not taken from the same location. The standard deviation values of radionuclides were found to be high due to the fact that the sample rocks taken from different locations had different chemical contents and differ in terms of their minimum and maximum values. This is an expected case in terms of statistics.

Table 4. Descriptive statistics of radionuclides and radiological indices.

	^{226}Ra	^{232}Th	^{40}K	Ra_{eq}	D	Iα	Iγ	H_{ex}	H_{in}	$AEDE_{indoor}$	$AEDE_{outdoor}$	AGDE	ELCR	AUI
N	30	30	30	30	30	30	30	30	30	30	30	30	30	30
Minimum	4.4	0.0	10.5	17.5	8.7	0.02	0.07	0.05	0.1	42.7	10.66	61.59	37.32	0.10
Maximum	752.3	386.8	3569.1	1503.4	691.6	3.8	5.3	4.1	6.1	3395.1	848.79	4779.93	2970.75	11.64
Mean ± SEM	148.5	148.1	1532.6	478.3	222	0.7	1.7	1.3	1.7	1089.7	272.43	1559.3	953.52	3.28
Std. Deviation	161.3	125.9	969.7	384.7	175.8	0.8	1.4	1.03	1.5	863.02	215.75	1220.73	755.14	2.95
Kurtosis	5.8	⁻0.7	⁻0.8	0.4	0.5	5.8	0.3	0.4	1.6	0.5	0.468	0.388	0.468	0.893
Skewness	2.1	0.7	⁻0.2	1.	0.9	2.1	0.9	1	1.3	0.9	0.929	0.889	0.929	1.197

The kurtosis values of the distributions of the radionuclides were found to be ^{226}Ra (5.8 > 3), ^{232}Th (−0.7), and ^{40}K (−0.8) in the descending order. While the distribution of ^{226}Ra had a leptokurtic shape, the distributions of ^{232}Th and ^{40}K had platykurtic shapes (Table 4, Figure 2).

The skewness range of (−2 < skewness < 2) covers 95% of the total area, while the skewness range of (−3 < skewness < 3) covers 99% of the total area. The skewness values of the radionuclides were found to be ^{226}Ra (−3 < 2.1 < 3), ^{232}Th (−2 < 0.7 < 2), and ^{40}K (−2 < −0.2 < 2) in the descending order. While the distribution of ^{226}Ra was found to have a right-skewed and asymmetrical shape, the distributions of ^{232}Th and ^{40}K could be assumed to have a normal distribution.

Figure 3 clearly indicates that the linear correlation coefficient between the effective ^{226}Ra content and ^{232}Th content was 0.9, pointing to the high strong linear dependency between both concentrations in the plutonic rocks.

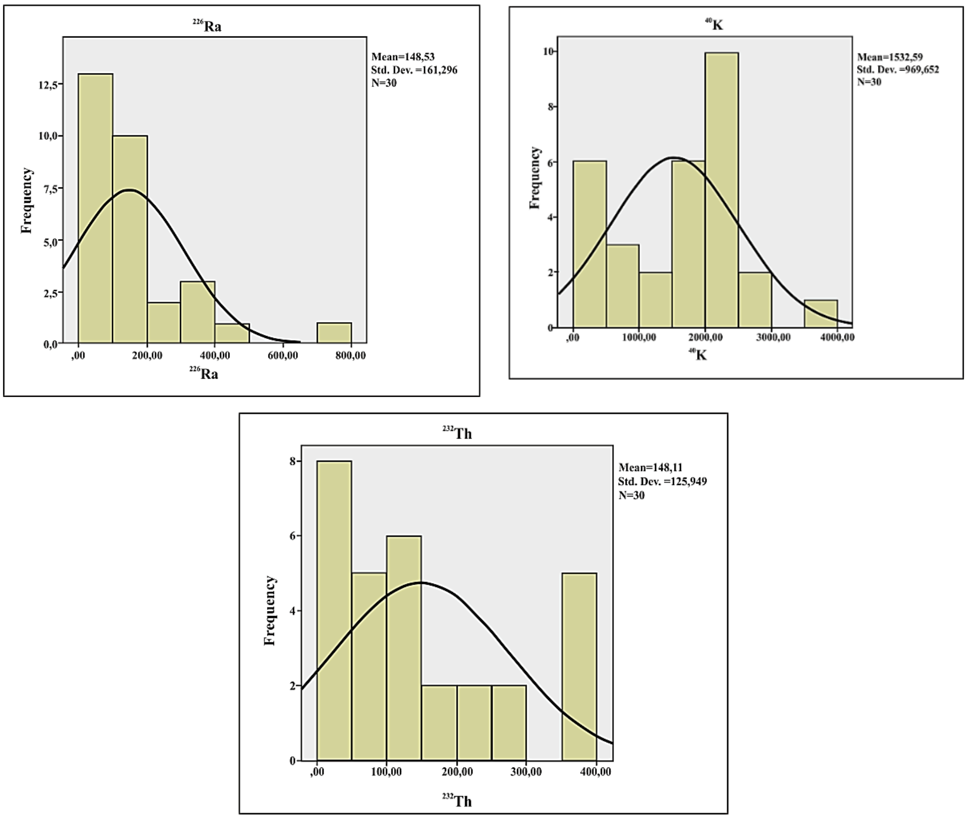

Figure 2. Frequency distributions of ^{226}Ra, ^{232}Th, and ^{40}K.

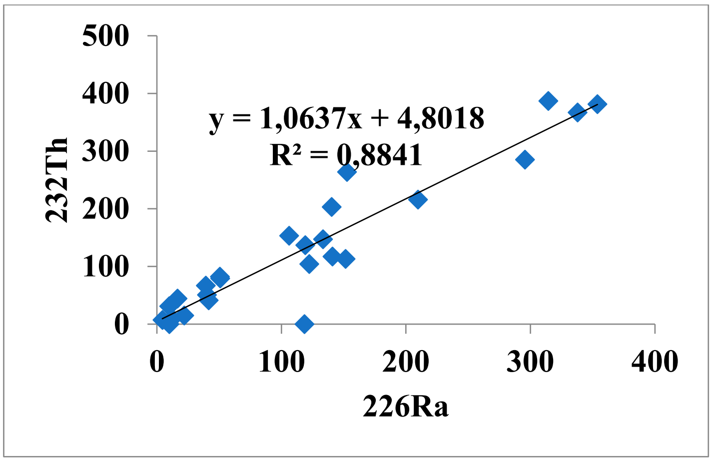

Figure 3. The relation between ^{226}Ra and ^{232}Th concentrations.

3.2.2. Correlation Analysis

A correlation analysis was performed to determine the relationship and similarity between all the data obtained. The normality of the data was tested before performing multivariate statistical analyses. The Kolmogorov–Smirnov and Shapiro–Wilk tests were used to test the normality of the distributions (Table 5). The significance values of all the data were calculated to be less than 0.05 (sig. < 0.05). Therefore, Spearman's correlation coefficient was used in the correlation analysis.

Table 5. Normality tests of all data.

	Kolmogorov–Smirnov [a]			Shapiro–Wilk		
	Statistic	**df**	**Sig.**	**Statistic**	**df**	**Sig.**
^{226}Ra	0.257	30	0.000	0.776	30	0.000
^{232}Th	0.150	30	0.083	0.889	30	0.005
^{40}K	0.190	30	0.007	0.912	30	0.017
Ra_{eq}	0.144	30	0.114	0.906	30	0.012
D	0.141	30	0.131	0.910	30	0.015
Iα	0.258	30	0.000	0.776	30	0.000
Iγ	0.134	30	0.176	0.913	30	0.018
H_{ex}	0.145	30	0.111	0.906	30	0.012
H_{in}	0.190	30	0.007	0.878	30	0.003
$AEDE_{indoor}$	0.141	30	0.131	0.910	30	0.015
$AEDE_{outdoor}$	0.141	30	0.131	0.910	30	0.015
AGDE	0.145	30	0.110	0.914	30	0.018
ELCR	0.141	30	0.131	0.910	30	0.015
AUI	0.222	30	0.001	0.869	30	0.002

[a] Lilliefors Significance Correction.

In general, the radionuclides have a positive correlation with the radiological parameters, which were obtained from the analysis of radionuclides (Table 6). In particular, while the radionuclides of ^{226}Ra and ^{232}Th have a positive correlation with the radiological parameters, ^{40}K has a lower positive correlation with these parameters. ^{40}K was observed to have a lower correlation with all other variables compared to the other radionuclides.

Table 6. Pearson correlation coefficients between the radioactive variables in the samples.

	^{226}Ra	**^{232}Th**	**^{40}K**	**Ra_{eq}**	**D**	**Iα**	**Iγ**	**H_{ex}**	**H_{in}**	**$AEDE_{indoor}$**	**$AEDE_{outdoor}$**	**AGDE**	**ELCR**	**AUI**
^{226}Ra	1													
^{232}Th	0.845 **	1												
^{40}K	0.641 **	0.729 **	1											
Ra_{eq}	0.939 **	0.963 **	0.804 **	1										
D	0.937 **	0.959 **	0.817 **	1.000 **	1									
Iα	1.000 **	0.845 **	0.641 **	0.939 **	0.937 **	1								
Iγ	0.931 **	0.962 **	0.822 **	1.000 **	1.000 **	0.931 **	1							
H_{ex}	0.939 **	0.963 **	0.803 **	1.000 **	1.000 **	0.939 **	0.999 **	1						
H_{in}	0.969 **	0.941 **	0.765 **	0.995 **	0.994 **	0.969 **	0.992 **	0.995 **	1					
$AEDE_{indoor}$	0.937 **	0.959 **	0.817 **	1.000 **	1.000 **	0.937 **	1.000 **	1.000 **	0.994 **	1				
$AEDE_{outdoor}$	0.937 **	0.959 **	0.817 **	1.000 **	1.000 **	0.937 **	1.000 **	1.000 **	0.994 **	1.000 **	1			
AGDE	0.933 **	0.958 **	0.826 **	0.999 **	1.000 **	0.933 **	1.000 **	0.999 **	0.992 **	1.000 **	1.000 **	1		
ELCR	0.937 **	0.959 **	0.817 **	1.000 **	1.000 **	0.937 **	1.000 **	1.000 **	0.994 **	1.000 **	1.000 **	1.000 **	1	
AUI	0.958 **	0.962 **	0.727 **	0.993 **	0.990 **	0.958 **	0.989 **	0.993 **	0.995 **	0.990 **	0.990 **	0.988 **	0.990 **	1

** Correlation is significant at the 0.01 level (2-tailed). * Correlation is significant at the 0.05 level (2-tailed).

Therefore, ^{226}Ra and ^{232}Th were found to have a more significant contribution to the radioactivity in the plutonic rocks. As a result, the variables that showed a positive correlation with the radioactivity parameters were interpreted to behave similarly and were of the same origin.

3.2.3. Factor Analysis

Factor analysis was applied to obtain significantly explained variables from the results of the analyses and calculations. The automatic factor selection tool of SPSS found one (1) factor with an eigenvalue greater than 1. However, the rotation sums of squared loadings method was applied to reveal the variance of the data and particularly ^{40}K, even it was very low; thus, the number of factors was selected as two (2) manually. In this context, two factors were extracted, and the cumulative value of variance explained was determined to be 98.7%. The results showed that the significant variance of the data was calculated very perfectly (Table 7).

Table 7. Total variance explained.

Component	Initial Eigenvalues			Extraction Sums of Squared Loadings			Rotation Sums of Squared Loadings		
	Total	% of Variance	Cumulative %	Total	% of Variance	Cumulative %	Total	% of Variance	Cumulative %
1	13.321	95.151	95.151	13.321	95.151	95.151	9.079	64.849	64.849
2	0.489	3.496	98.647	0.489	3.496	98.647	4.732	33.799	98.647

Extraction Method: Principal Component Analysis.

Principal component analysis (PCA) was performed after factor analysis. According to the results of the rotated component matrix data, two components were determined (Table 8). The first factor was determined to consist of ^{226}Ra, ^{232}Th, Ra_{eq}, D, Iα, Iγ, Hex, H_{in}, $AEDE_{indoor}$, $AEDE_{outdoor}$, AGDE, ELCR, and AUI, and their total variance was found to be 95.1%. The second factor was determined to consist of ^{40}K with a total variance value of 3.5%. The radionuclide of ^{40}K, which constitutes a separate component, is completely independent of the variables representing the other component. With its percentage of 3.5% in the grand total, ^{40}K has a high effect on the total variance. It has an important place in the statistical evaluation of the data. This finding indicates that ^{40}K has a different effect than ^{226}Ra and ^{232}Th. It is considered that the radionuclides of ^{226}Ra and ^{232}Th are influenced by granitic rocks, as well as ^{40}K being affected by rock alterations, and clayey rocks have more effect on this radionuclide.

Table 8. Rotated factor loadings and explained variance for variables in the samples.

Variables	Component	
	1	2
^{226}Ra	0.929	0.325
^{232}Th	0.767	0.569
^{40}K	0.332	0.926
Ra_{eq}	0.813	0.582
D	0.802	0.597
Iα	0.929	0.325
Iγ	0.794	0.607
H_{ex}	0.813	0.582
H_{in}	0.858	0.513
$AEDE_{indoor}$	0.802	0.597
$AEDE_{outdoor}$	0.802	0.597
AGDE	0.793	0.609
ELCR	0.802	0.597
AUI	0.874	0.483
% of variance explained	95.151	3.496

Extraction Method: Principal Component Analysis.
Rotation Method: Varimax with Kaiser Normalization. [a]

[a] Rotation converged in 3 iterations.

After analyzing the Scree Plot of the data used in the factor analysis, it can be seen that the data is flattened after the second factor; therefore, extraction of two factors from these data seems to be appropriate (Figure 4).

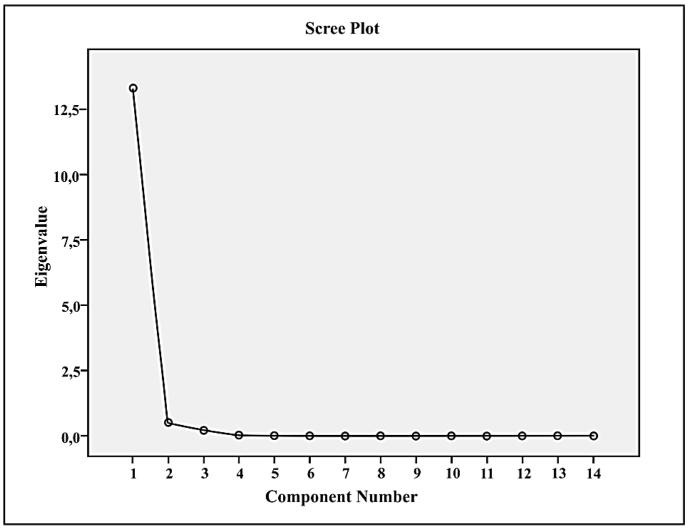

Figure 4. Scree plot of the principal component analysis.

According to the principal component analysis, ^{226}Ra and ^{232}Th radionuclides were found to have a very high effect on the radiological parameters; this finding seemed to be compatible with the correlation analysis. ^{40}K showed a different behavior compared to the other radionuclides and indices and seemed to be distant from them (Figure 5).

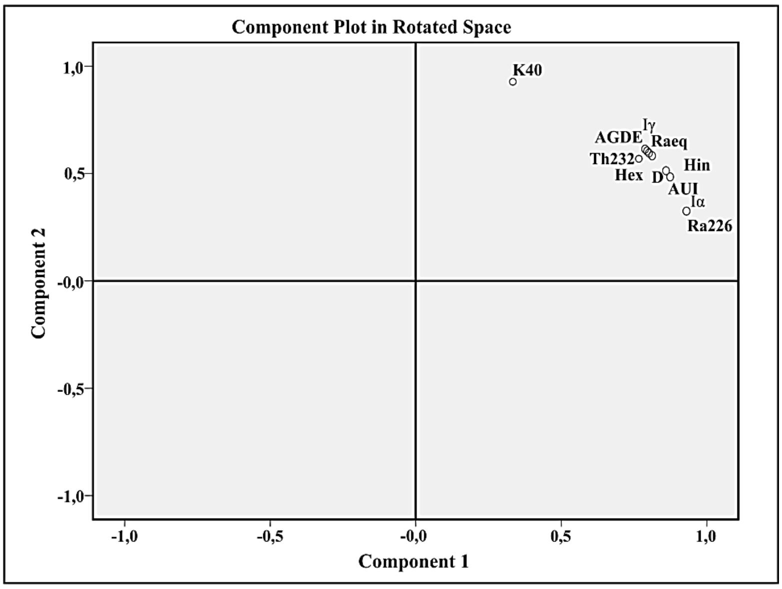

Figure 5. Component plot in the varimax-rotated space, component 1 (95.1%) and component 2 (3.5%).

3.2.4. Cluster Analysis (CA)

The Wards method was used in the hierarchical cluster analysis and the Q-mode cluster showed an arbitrary similarity level of 50%. Two (2) groups were determined in the dendrogram of a total of 30 samples (Figure 6). The samples showing similarities among themselves were determined. The samples of N9-F-29, N11-F-34, and N15-E-18 together with N13-E-3 and N14-E-14, which were connected to them externally, formed the first dendrogram. The second dendrogram consisted of the samples of N27-SR-5, N29-SR-12, N6-KR-3, N16-ST-1, N20-ST-87, N30-SR-18, N18-ST-59, N7-KR-4, N28-SR-11, N23-KP-2, N17-ST-52, N19-ST-80, N5-KR-1, N8-KR-7, and N10-F-31, which were connected to them externally. The samples in the same dendrogram showed similar characteristics.

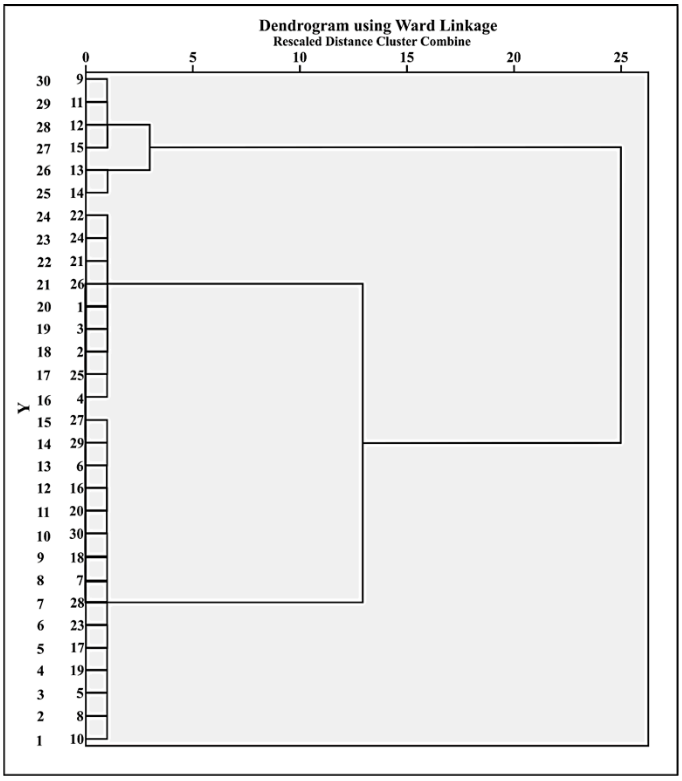

Figure 6. The clustering of radioactive variables.

3.3. Comparison with Other Countries

Before comparing the average values of plutonic rock samples collected from the study area with the world averages, muscovite schist sample (N6-KR-3) as a metamorphic rock, aplite sample (N13-E-3) as a dike, and pegmatite rock samples (N14-E-14, N18-ST-59, N23-KP-2) were excluded from the dataset in the calculation of the average values since they increased the grand mean significantly. The values of ^{226}Ra (148.53), ^{232}Th (148.11), and ^{40}K (1532.59) seemed to have an abnormally negative impact on the grand mean of the region. In particular, the aplite sample No. N13-E-3 collected from the Camlik region had the highest ^{40}K value while the pegmatite rock sample No. N14-E-14 had the highest ^{226}Ra value. All the data about ^{40}K were grouped into four equal classes (10.5–624; 624–1694.9; 1695–2582.4; 2582.4–3569.1), and star figures were created from these new data; then, they were marked on the site location map (Figure 1).

The mean values of granite, metagranite, and chlorite schist samples were taken into consideration to evaluate the situation using similar samples from various countries in the world (Table 9). The average ^{226}Ra (119.7), ^{232}Th (132.1), and ^{40}K (1295.3) values were compared with the world averages of the granite samples in terms of the average natural radioactivity behavior of these rocks. Additionally, the samples were compared with the average values of the natural granite samples from different countries and different regions of Turkey, including the commercial ones and the imported ones.

Table 9. Concentrations of ^{226}Ra, ^{232}Th, and ^{40}K in different plutonic rock samples.

Location		**Specific activity (Bq kg^{-1})**			**References**
		^{226}Ra	**^{232}Th**	**^{40}K**	
Turkey	Western and Central Sakarya Zone [1]	119.7	132.1	1295.3	This Study
World average	Granite samples	78	111	1104	[14]
Brazil	commercial [2]	82.5	227	1109.5	[15]
	imported[3]	69.6	75.6	580	[16]
China	commercial [2]	102	94	632	[17]
	commercial [2]	88	114	1270	[18]
	commercial [2]	90	116	969	[19]
Cyprus	commercial [2]	77	143	1215	[20]
Egypt	South Eastern Desert [1]	121.3	82.2	840	[21]
	Abu Dabbab Mine [1]	45.8	29.8	619.7	[22]
Greece	commercial [2]	74	85	881	[23]
	commercial [2]	64	81	1104	[25]
Iran	commercial [2]	44.5	77.4	1017.2	[26]
Italy	imported [2]	59.8	92.3	1141.2	[27]
Japan	commercial [2]	43	72	1004	[28]
Jordan	Amman [1]	41.5	58.4	497	[29]
Nigeria	commercial [2]	51.1	88	1433	[30]
Palestine	commercial [2]	71.0	82	780.8	[31]
Saudi Arabia	Al Madinah [1]	33.25	51.45	1334	[7]
Spain	commercial [2]	84	42	1138	[32]
Turkey	commercial [2]	71	80	965	[33]
	imported [3]	93.4	124.8	1050	[34]
	Western Anatolia	58	90	1097	[24]
	commercial [1]	88	95	1055	[35]
	Kutahya [1]	56.4	25.9	538.4	[36]
	Ezine [1]	175	205	1172	[54]
	Egrigoz [1]	55	76	1111	[55]
	commercial [2]	61	60	851	[36]
USA	commercial [2]	31	61	1210	[37]
Yemen	Juban [1]	54	127	1743	[38]

[1] natural rocks; [2] decorative rocks or ornamental stones; [3] imported granites.

Considering the average values of granite, metagranite, and chlorite schist samples, ^{226}Ra (119.7), ^{232}Th (132.1), and ^{40}K (1295.3) values were found to exceed the world averages (Table 9). The ^{226}Ra value of the samples seemed to be higher than all other samples except for those from the South Eastern Desert (Egypt), Ezine (Turkey), and commercial ones (China). The ^{232}Th value was determined to be higher than all other samples, except for commercial ones (China). The ^{40}K value showed higher values than all other samples, except for those from Al Madinah (Saudi Arabia) and Juban (Yemen).

Likewise, the average radioactivity values of the plutonic rock samples from Camlik, Sogukpinar, Karacabey, and Sogut (except for ^{232}Th) were found to be higher than the world averages. Particularly, the ^{40}K values in these regions were higher than those of samples from various countries in the world. The average radioactivity values of the plutonic rock samples from Ericek and Kapanca were found to be lower than the world averages and those of samples from other regions (Figure 7).

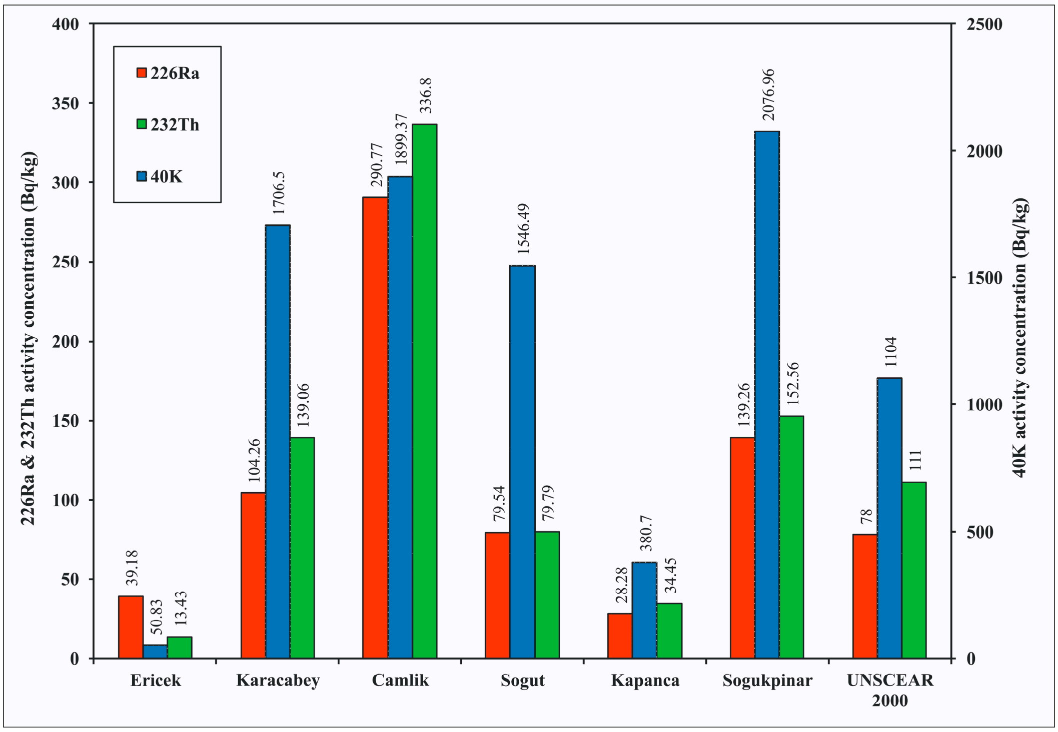

Figure 7. The activity concentration of ^{226}Ra, ^{232}Th, and ^{40}K in the plutonic rock samples.

4. Conclusions

The radiological levels of the plutonic rock samples from various regions in the Sakarya Zone were measured and their radioactivity parameters were calculated; then, all data were interpreted using multivariate statistical methods.

Considering the average radioactivity concentrations of granite and metagranite, which are plutonic rocks, and chlorite schist, which is a metamorphic rock, the abundance order was determined to be ^{40}K (1295.3 Bq kg^{-1}) > ^{232}Th (132.1 Bq kg^{-1}) > ^{226}Ra (119.7 Bq kg^{-1}). Therefore, the plutonic rocks should be identified in similar studies, and dikes should not be taken into consideration in the calculation of the grand mean.

The average values of the absorbed dose rate (D), radium equivalent activity (Ra_{eq}), external hazard index (H_{ex}), internal hazard index (H_{in}), the annual effective dose equivalent values of $AEDE_{indoor}$ and $AEDE_{outdoor}$, the annual gonadal dose equivalent (AGDE), excess lifetime cancer risk ($ELCR_{outdoor}$), and activity utilization index (AUI) were found to be 222, 478.3, 1.3, 1.7, 1089.7, 272.4, 1559.3, 953.5, and 3.3, respectively. All average values were found to exceed world limit values. The averages of the alpha index ($I\alpha$) and gamma index ($I\gamma$) values were found to be 0.7427 and 1.7463, respectively. Therefore, the radiological effect was determined to exceed the value that can be tolerated ($I\gamma < 0.5$). The results of the AUI calculations revealed that there was external gamma radiation from the surface materials.

According to the descriptive statistics applied as part of the multivariate statistical analyses, the skewness values of the radionuclides were found to be ^{226}Ra ($-3 < 2.1 < 3$), ^{232}Th ($-2 < 0.7 < 2$), and ^{40}K ($-2 < -0.2 < 2$). The distribution of ^{226}Ra was found to have a positively right-skewed and asymmetrical shape while the distribution of ^{232}Th had a positively right-skewed symmetrical shape, and ^{40}K had a negatively right-skewed and symmetrical shape. The kurtosis values of the distributions of the radionuclides were found to be ^{226}Ra ($5.8 > 3$), ^{232}Th (-0.7), and ^{40}K (-0.8) in the descending order. The ^{226}Ra radionuclide had a sharply peaked and the highest distribution.

Kolmogorov–Smirnov and Shapiro–Wilk normality tests were performed, and the significance values were found to be less than 0.05 (sig. < 0.05). Therefore, it was decided that the data did not have a normal distribution, and Spearman's correlation coefficient method was performed. A positive correlation was found between ^{226}Ra, ^{232}Th, and the radiological parameters. It was interpreted that they had a higher radioactivity effect. However, ^{40}K did not show a similar correlation level. The findings also reveal that the radionuclides of ^{226}Ra and ^{232}Th are geologically affected by granitic rocks. On the other hand, ^{40}K was affected by clayey rocks formed by the alteration of granitic rocks.

Factor analysis resulted in two factors with a cumulative value of 98.7%. While one of the factors represents ^{40}K (3.5%), the other factor represents all remaining variables (95.2%). The diagram clearly shows that ^{40}K is positioned in a different location from other variables. Moreover, the Scree Plot of the variables is flattened after the second component.

Two (2) hierarchical groups were obtained from the Q-mode cluster at the arbitrary similarity level of 50%. While the first group consists of N9-F-29, N11-F-34, N15-E-18, N13-E-3, and N14-E-14, the second group consists of N22-KP-1, N24-KP-8, N21-ST-89, N26-KP-12, N1-ER-2, N3-ER-4, N2-ER-3, N25-KP-11, N4-ER-5, N27-SR-5, N29-SR-12, N6-KR-3, N16-ST-1, N20-ST-87, N30-SR-18, N18-ST-59, N7-KR-4, N28-SR-11, N23-KP-2, N17-ST-52, N19-ST-80, N5-KR-1, N8-KR-7, and N10-F-31. The first group, which showed higher values, is prominent.

The radiological values of the samples from the Sakarya Zone are higher than the world average. The ^{226}Ra value was found to be lower than the values of the samples from the South Eastern Desert (Egypt), Ezine (Turkey), and commercial ones (China). The ^{232}Th value was found to be lower than that of the commercial sample (China), and the ^{40}K value was found to be lower than the values of the samples from Al Madinah (Saudi Arabia) and Juban (Yemen). However, the values were found to be higher than other samples from various regions of the world.

The average radioactivity values of Camlik, Sogukpinar, Karacabey, and Sogut (except for ^{232}Th) were observed to be higher than the world averages. The average ^{40}K value was higher than the world average, as well as the values of samples from various countries in the world.

The samples exceeding the limit values are not suitable for use as a building material. Inhalation of radon and its products may lead to health problems. The AGDE calculations revealed a significant finding that the radiation received by the reproductive organs (gonads) of the population exceeds the annual gonadal dose equivalent. According to the $ELCR_{outdoor}$ calculations, the lifetime cancer risk for up to 70 years due to land use is high. Therefore, it will be appropriate to carry out a follow-up on the rocks used as products quickly and effectively. The scope of the production of these rocks, their marketing, and use as a building material should be limited.

Author Contributions: Conceptualization, F.Y., N.I. and M.G.Y.; methodology, M.D., S.F.O., A.G.; software, F.Y.; validation, N.I. and M.G.Y.; formal analysis, F.Y., N.I., A.G.; investigation, A.K.; resources, M.G.Y. and A.G.; data curation, F.Y.; writing-original draft preparation, F.Y., N.I. and M.G.Y.; writing-review and editing, M.D. and A.K.; visualization, M.G.Y. and A.G.; supervision, N.I. and M.G.Y.; project administration, N.I.; funding acquisition, N.I. All authors have read and agreed to the published version of the manuscript.

Funding: This research received no external funding.

Acknowledgments: The corresponding author, Nurdane Ilbeyli, extends her appreciation to the Scientific Research Projects Coordination Unit at Akdeniz University for funding the Ra, Th, K analyses of the rocks by the Research Groups Program (Project Number: FBA-2015-652).

Conflicts of Interest: The authors declare no conflict of interest.

References

1. Beck, H.L. *Exposure Rate Conversion Factors for Radionuclides Deposited on the Ground, Report no.EML-378*; Department of Energy: New York, NY, USA, 1980.
2. Onargan, T.; Gur, F.; Kaya, E.; Guneri, S. Assessment of natural radioactivity in commercial granites used in Turkey. *J. Environ. Sci. Health Part A* **2012**, *47*, 1825–1830. [CrossRef]
3. Ramassay, V.; Dheenathayalu, M.; Ravisankar, R.; Ponnusamy, V. Natural radioactivity measurements in Beach-rock samples of South-East Coast of Tamilnadu, India. *Radiat. Prot. Dosim.* **2004**, *111*, 229–235. [CrossRef]
4. Rati, V.; Mahur, A.; Sonkawade, R.; Suhail, M.; Azam, A.; Prasad, R. Evaluation and analysis of 226Ra, 232Th, 40K and radon exhalation rate in various grey cements. *Indian J. Pure Appl. Phys.* **2010**, *48*, 473–482.

5. Saito, K.; Jacop, P. Gamma ray fields in the air due to sources in the ground. *Radiat. Prot. Dosim.* **1995**, *58*, 29–45.
6. Agbalagba, E.O.; Avwiri, G.O.; Chad-Umoreh, Y.E. Gamma-spectroscopy measurement of natural radioactivity and assessment of radiation hazard indices in soil samples from oil fields environment of Delta State, Nigeria. *J. Environ. Radioact.* **2012**, *109*, 64–70. [CrossRef]
7. Mohamed, R.I.; Algamdi, S.K.; Al-Shamani, N.S. Evaluation of radionuclide concentrations and associated radiological hazard in marble indices and granite used as building materials in Al-Madinah Al-Munawarah. *J. Taibah Univ. Sci.* **2016**, *10*, 369–374. [CrossRef]
8. El-Gamal, H.; El-Haddad, M. Estimation of Natural Radionuclides and Rare Earth Elements Concentration of the Rocks of Abu Khuruq Ring Complex, Egypt. *Symmetry* **2019**, *11*, 1041. [CrossRef]
9. Nyamsari, D.G.; Yalcin, M.G.; Wolfson, I. Alteration, Chemical Process and Parent Rock of Haléo-Danielle Plateau Bauxite, Adamawa–Cameroon. *Lith. Miner. Res.* **2020**, *55*, 231–243. [CrossRef]
10. Ozmen, S.F.; Boztosun, I.; Yavuz, M.; Tunc, M.R. Determination of gamma radioactivity levels and associated dose rates of soil samples of the Akkuyu/Mersin using high-resolution gamma-ray spectrometry. *Radiat. Prot. Dosim.* **2013**, *158*, 461–465. [CrossRef]
11. Monica, S.; Visnu Prasad, A.K.; Soniya, S.R.; Jojo, P.J. Estimation of indoor and outdoor effective doses and lifetime cancer risk from gamma dose rates along the coastal regions of Kollam district, Kerala. *Radiat. Prot. Environ.* **2016**, *39*, 38–43.
12. Qureshi, A.A.; Manzoor, S.; Younis, H.; Shah, K.H.; Ahmed, T. Assessment of Radiation Dose and Excessive Life-Time Cancer Risk from the Bunair Granite, Northern Pakistan. *Radiat. Prot. Dosim.* **2018**, *178*, 143–151. [CrossRef] [PubMed]
13. UNSCEAR, United Nations Scientific Committee on the Effects of Atomic Radiation. *Sources and Biological Effects of Ionizing Radiation*; United Nations: New York, NY, USA, 1988.
14. UNSCEAR, United Nations Scientific Committee on the Effects of Atomic Radiation. *Sources, Effects and Risks of Ionizing Radiation, Report to the General Assembly with Annex B: Exposures from Natural Sources of Radiation*; United Nations: New York, NY, USA, 2000.
15. Anjos, R.M.; Juri Ayub, J.; Cid, A.S.; Cardoso, R.; Lacerda, T. External gamma-ray dose rate and radon concentration in indoor environments covered with Brazilian granites. *J. Environ. Radioact.* **2011**, *102*, 1055–1061. [CrossRef]
16. Moura, C.L.; Artur, A.C.; Bonotto, D.M.; Guedes, S.; Martinelli, C.D. Natural radioactivity and radon exhalation rate in Brazilian igneous rocks. *J. Appl. Radiat. Isot.* **2011**, *69*, 1094–1099. [CrossRef] [PubMed]
17. Mao, Y.; Liu, Y.; Fu, Y.; Lin, L. Physical models and limits of radionuclides for decorative building materials. *Health Phys.* **2006**, *90*, 471–476. [CrossRef]
18. Xinwei, L.; Lingqing, W.; Xiaodan, J. Radiometric analysis of Chinese commercial granites. *J. Radioanal. Nucl. Chem.* **2006**, *267*, 669–673. [CrossRef]
19. Gbadamosi, M.R.; Afolabi, T.A.; Banjoko, O.O.; Ogunneye, A.L.; Abudu, K.A.; Ogunbanjo, O.O.; Jegede, D.O. Spatial distribution and lifetime cancer risk due to naturally occurring radionuclides in soils around tar-sand deposit area of Ogun State, southwest Nigeria. *Chemosphere* **2018**, *193*, 1036–1048. [CrossRef]
20. Tzortzis, M.; Tsertos, H.; Christofides, S.; Christodoulides, G. Gamma measurements and dose rates in commercially used tiling rocks (granites). *J. Environ. Radioact.* **2003**, *70*, 223–235. [CrossRef]
21. El-Gamal, H.; Sidique, E.; El-Haddad, M.; Farid, M.A. Assessment of the natural radioactivity and radiological hazards in granites of Mueilha area (South Eastern Desert, Egypt). *Environ. Earth Sci.* **2018**, *77*, 19. [CrossRef]
22. Heikal, S.; Gomaa, S.R.; Abd El Monsef, M.; Taha, A.A.; Top, G.; Mahmoud, K.R.; El-Mansi, M.M. Insight on Radiological Risk Assessment and its Statistical Evaluations for Abu Dabbab Albite Granite Mining Area, Central Nubian Shield, Egypt. *Arab J. Nucl. Sci. Appl.* **2018**, *51*, 143–167.
23. Papadopoulos, A.; Christofides, G.; Koroneos, A.; Papadopoulou, L.; Papastefanou, C.; Stoulos, S. Natural radioactivity and radiation index of the major granitic plutons in Greece. *J. Environ. Radioact.* **2013**, *124*, 227–238. [CrossRef]
24. Papadopoulos, A.; Altunkaynak, S.; Koroneos, A.; Unal, A.; Kamaci, O. Distribution of natural radioactivity and assessment of radioactive dose of Western Anatolian plutons, Turkey. *Turk. J. Earth Sci.* **2016**, *25*, 434–455. [CrossRef]
25. Pavlidou, S.; Koroneos, A.; Papastefanou, C.; Christofides, G.; Stoulos, S.; Vavelides, M. Natural radioactivity of granites used as building materials. *J. Environ. Radioact.* **2006**, *89*, 48–60. [CrossRef] [PubMed]

26. Abbasi, A. Calculation of gamma radiation dose rate and radon concentration due to granites used as building materials in Iran. *Radiat. Prot. Dosim.* **2013**, *155*, 335–342. [CrossRef] [PubMed]
27. Michael, F.; Parpottas, Y.; Tsertos, H. Gamma Radiation Measurements and dose rates in commonly used building materials in Cyprus. *Radiat. Prot. Dosim.* **2010**, *142*, 282–291. [CrossRef]
28. Iwaoka, K.; Hosoda, M.; Tabe, H.; Ishikawa, T.; Tokonami, S.; Yonehara, H. Activity concentration of natural radionuclides and radon and thoron exhalation rates in rocks used as decorative wall coverings in Japan. *Health Phys.* **2013**, *104*, 41–50. [CrossRef]
29. Hamideen, M.S.; Bdair, O.M.; Chandrasekaran, A.; Saleh, H.; Elimat, Z.M. Multivariate statistical investigations of natural radioactivity and radiological hazards in building materials mainly used in Amman Province, Jordan. *Int. J. Environ. Anal. Chem.* **2020**, *100*, 189–203. [CrossRef]
30. Ademola, J.A. Occupational Exposure Due to Naturally Occurring Radionuclide Material in Granite Quarry Industry. *Radiat. Prot. Dosim.* **2012**, *148*, 297–300. [CrossRef]
31. Thabayneh, K.M. Measurement of Natural Radioactivity and Radon Exhalation Rate in Granite Samples Used in Palestinian Buildings. *Arab. J. Sci. Eng.* **2013**, *38*, 201–207. [CrossRef]
32. Guillen, J.; Tejado, J.J.; Baeza, A.; Corbacho, J.A.; Munoz, J.G. Assessment of radiological hazard of commercial granites from Extremadura (Spain). *J. Environ. Radioact.* **2014**, *132*, 81–88. [CrossRef]
33. Angi, O.S.; Yavuz, O.; Yalcin, T.; Ciftci, E. Mineralogy-induced radiological aspects with characterization of commercial granites exploited in Turkey. *Bull. Eng. Geol. Environ.* **2016**, *76*, 507–522. [CrossRef]
34. Cetin, E.; Altinsoy, N.; Orgun, Y. Natural radioactivity levels of granites used in Turkey. *Radiat. Prot. Dosi.* **2012**, *151*, 299–305. [CrossRef] [PubMed]
35. Turhan, S. Estimation of possible radiological hazards from natural radioactivity in commercially-utilized ornamental and countertops granite tiles. *Ann. Nucl. Energy* **2012**, *44*, 34–39. [CrossRef]
36. Sahin Bal, S. The determination of concentrations of radioisotopes in some granite samples in Turkey and their radiation hazards. *Rad. Eff. Def. Sol.* **2018**, *173*, 353–366. [CrossRef]
37. Kitto, M.E.; Haines, D.K.; Menia, T.A. Assessment of gamma-ray emissions from natural and manmade decorative stones. *J. Radioanal. Nucl. Chem.* **2009**, *282*, 409–413. [CrossRef]
38. Abd El-mageed, A.I.; El-Kamel, A.H.; Abbady, A.; Harb, S.; Youssef, A.M.M.; Saleh, I.I. Assessment of natural and anthropogenic radioactivity levels in rocks and soil in the environments of Juban town in Yemen. *Radiat. Phys. Chem.* **2011**, *80*, 710–715. [CrossRef]
39. Okay, A. Metamorphic Evolution of the Pre-Jurassic Basement of the Sakarya Zone. *Geol. Congr. Turk.* **2011**, *64*, 215–216.
40. Yilmaz, M.; Ozmen, S.F. Radiologic Risk Assessment of Fish Feed and Feed Raw Materials. *Aquac. Res.* **2020**, *51*, 2190–2196. [CrossRef]
41. Ozmen, S.F.; Cesur, A.; Boztosun, I.; Yavuz, M. Distribution of natural and anthropogenic radionuclides in beach sand samples from Mediterranean Coast of Turkey. *Radiat. Phys. Chem.* **2014**, *103*, 37–44. [CrossRef]
42. Unal, S.; Yalcin, M.G.; Ocak, S.; Yalcin, R.; Ozmen, S.F. Computation of gamma radioactivity of natural rocks in the vicinity of Antalya province and its effect on health. *Kerntechnik* **2018**, *83*, 112–120. [CrossRef]
43. Alam, M.N.; Chowdhury, M.I.; Kamal, M.; Ghose, S.; Islam, M.N.; Mustafa, M.N.; Miah, M.M.H.; Ansary, M.M. The 226Ra, 232Th and 40K activities in beach sand minerals and beach soils of Cox's Bazar, Bangladesh. *J. Environ. Radioact.* **1999**, *46*, 243–250. [CrossRef]
44. Beretka, J.; Mathew, P.J. Natural radioactivity of Australian building materials, industrial wastes and by-products. *Health Phys.* **1985**, *48*, 87–95. [CrossRef]
45. Mamont-Ciesla, K.; Gwiazdowski, B.; Biernacka, M.; Zak, A. Radioactivity of building materials in Poland. In *Natural Radiation Environment*; Halsted Press: New York, NY, USA, 1982; p. 551.
46. Jallad, K.N. Radiation hazard indices and excess lifetime cancer risk in sand from the northern and eastern regions of Kuwait. *Environ. Earth Sci.* **2016**, *75*, 1–10. [CrossRef]
47. Mohammed, R.S.; Ahmed, R.S. Estimation of excess lifetime cancer risk and radiation hazard indices in southern Iraq. *Environ. Earth Sci.* **2017**, *76*, 303. [CrossRef]
48. Ravisankar, R.; Vanasundari, K.; Suganya, M.; Raghu, Y.; Rajalakshmi, A.; Chandrasekaran, A.; Sivakunar, S.; Chandramohan, J.; Vijayagopal, P.; Venkatraman, B. Multivariate statistical analysis of radiological data of building materials used in Tiruvannamalai, Tamilnadu, India. *Appl. Radiat. Isot.* **2014**, *85*, 114–127. [CrossRef]

49. Heikal, M.T.S.; Top, G. Assessment of radioactivity levels and potential radiation health hazards of Madsus granites and associated dikes nearby and around Ruwisat village, South Sinai, Egypt. *J. Afr. Earth Sci.* **2018**, *146*, 191–208. [CrossRef]
50. Yalcin, M.G.; Unal, S. Natural radioactivity levels and associated radiation hazards in ophiolites around Tekirova, Kemer, and Kumluca Touristic Regions in Antalya, Turkey. *J. Radioanal. Nucl. Chem.* **2018**, *316*, 321–330. [CrossRef]
51. Nyamsari, D.G.; Yalcin, F.; Mboh, M.T.; Alfred, F.G.; Yalcin, M.G. Natural radioactive risk assessment in top soil and possible health effect in Minim and Martap villages, Cameroon: Using radioactive risk index and statistical analysis. *Kerntechnik* **2019**, *84*, 115–122. [CrossRef]
52. Morsy, Z.; El-wahab, M.A.; El-Faramawy, N. Determination of natural radioactive elements in Abo Zaabal, Egypt by means Gamma Spectroscopy. *Ann. Nucl. Energy* **2012**, *44*, 8–11. [CrossRef]
53. Ramasamy, V.; Sundarrajan, M.; Paramasivam, K.; Meenakshisundaram, V.; Suresh, G. Assessment of spatial distribution and radiological hazardous nature of radionuclides in high background area, Kerala, India. *Appl. Radiat. Isot.* **2013**, *73*, 21–31. [CrossRef] [PubMed]
54. Orgun, Y.; Altınsoy, N.; Sahin, S.Y.; Gungor, Y.; Gultekin, A.H.; Karahan, G.; Karacik, Z. Natural and anthropogenic radionuclides in rocks and beach sands from Ezine region (Canakkale), Western Anatolia, Turkey. *Appl. Radiat. Isot.* **2007**, *65*, 739–747. [CrossRef] [PubMed]
55. Canbaz, O.B.; Yaprak, G.; Cam, N.F.; Candan, O. A radiological Survey of the Egrigoz Granitoid, Western Anatolia/Turkey. *Radiat. Prot. Dosi.* **2015**, *164*, 510–518. [CrossRef] [PubMed]